Mapping of Middle Miocene Reservoir Sands and Subtle Faults to Understand Reservoir Compartmentalization in Erawan Field of Pattani Basin, Gulf of Thailand

Chatchai Inthana

Petroleum Geoscience Program, Department of Geology, Faculty of Science, Chulalongkorn University, Bangkok 10330, Thailand
Corresponding author email: aekexp@outlook.com

Abstract

Erawan field is one of the oldest hydrocarbon producing fields of the Pattani basin within the Gulf of Thailand. Reservoirs in this field are Middle Miocene fluvial sands. These sands are crosscut by set of faults, which are oblique to regional north-south oriented faults. These faults are difficult to map on conventional full spectrum seismic data. The purpose of this study is to map these subtle faults and sand distribution in the area. I integrated various geophysical attributes and techniques such as RMS, semblance, post-stack inversion and spectral decomposition to map faults and sand distribution. Time slices of iso-frequency volumes in the range of 24-28 Hz shows NW-SE and SW-NE oriented discontinuities. Similar discontinuities were also observed on semblance horizon slices. These are oblique to the regional N-S faults and at some places, they crosscut the regional faults on map view. On filtered seismic vertical sections with band limited frequency of 20-30 Hz, they penetrate sometimes to basement. These are interpreted as faults related with graben shifts/transfer zones. Rock physics analysis shows that acoustic impedance can discriminate high porosity sands and high gas saturated clean sands. Suitable cutoff for sand can detect sand bodies in the zone of interest. Very low acoustic impedance values are distributed along both regional and oblique faults and these may be related with gas-saturated zones. Therefore, mapping of these oblique discontinuities are critical for recognition of reservoir compartments. The suggested workflow can reduce the exploration risk in the area.

Keywords: Middle Miocene fluvial sands, post-stack inversion, Spectral decomposition, Iso-frequency volumes, Oblique discontinuities

1. Introduction

The Erawan field is located on the western flank of the Pattani Basin within the Gulf of Thailand (Figure 1). The reservoirs in these basins are Lower to Middle Miocene fluvial channels and overbank sands and these reservoirs are dissected by the post-depositional faulting (Morley and Racey, 2011). There are many tiny inseparably spaced sealing faults, which segregate the sand reservoirs and hard to map on the conventional full spectrum seismic data.

These faults systems are at oblique angle to the regional N-S normal faults and associated with graben shifts or transfer zones relevant with changes in dip of graben area and diagonal map pattern of the regional N-S normal faults (Kornsawan and Morley, 2002). Many wells that were drilled on the structures along the faults normally encountered different lithologies. Moreover, prediction for reservoir fluids is not easy based on only amplitudes of seismic data. Therefore, because of these structural and stratigraphic complexities, it is important to suggest a workflow, which can reduce exploration risk.

2. Regional Geology

Pattani basin is located in the central of the Gulf of Thailand and covers an area at the junction of Shan-Thai craton and Indonesian craton (Crossley, 1990). According to Jardine (1997), Pattani basin formed due to crustal extension caused by northward movement and collision of the Indian plate into Eurasia plate and the tectonic activity leading to structural evolution stage of initial rift, syn-rift and post-rift. There are several structurally complex extensional basins and strike-slip fault systems. Three Pagodas fault extends from Myanmar border and appears to extend into the northern part of the Gulf of Thailand. The northeast-southwest trending of Ranong fault cut across peninsular Thailand and perhaps extends into the northern part of the Gulf of Thailand and major fault systems bound a series of north-south trending structures. The fault pattern appears have been strongly influenced by pre-existing basement trends due to complex transfer zones associated with fault-linkage geometries (Kornsawan and Morley, 2002).

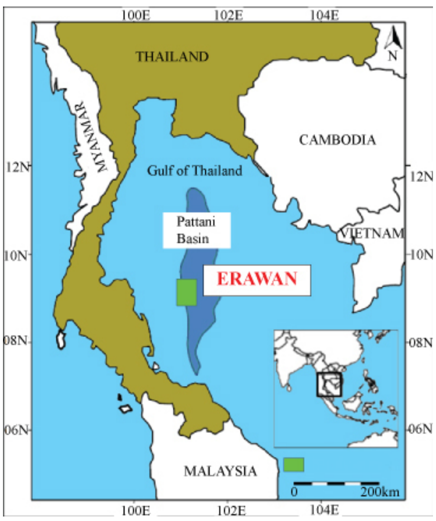

Figure 1. Map of study area (green box) in Pattnai Basin, Gulf of Thailand.

The Pattani basin fill is retained of non-marine and marginal marine siliciclastic sediments of Tertiary age that are more than 7,620 meters of thickness (Morley and Racey, 2011). Sequence 1: Oligocene, this sequence is considered to be a complex of syn-rift strata. It is a mixture of alluvial beds on the half-graben margins that grade into lacustrine beds in the half-graben centers. Sequence 2: Early Miocene, this sequence is consists of interbedded red and grey shale, sandstone and coal make up this sequence. Mostly it was deposited in fluvial floodplain and delta environment. Sequence 3: Early Middle Miocene, this sequence is mainly grey shale and coal deposit due to transgressive fluvial to marginal marine environment. However, sandstone in this sequence may not be restricted simply to fluvial meander belt, but could possibly deposit in some widely developed marginal marine environment. Sequence 4: middle-late Middle Miocene there are more fluvial red beds and occasional coal bed. This sequence was deposited by avulsion of meander belt system in fluvial environment. The upper sequence contact is clearly marked by a major regional unconformity known as the Middle Miocene Unconformity (MMU).

3. Methodology

RMS attribute

RMS (root mean square) amplitude attribute were applied along the interpreted horizons in order to map sand distribution. I performed windows of different intervals such 5, 10 and 20 msec centered on interpreted horizons.

Semblance

I performed this tool for measure of similarity of trace or continuity of the seismic waveform in the specific window. The purpose is to highlights lateral and vertical stratigraphic and structure changes.

Spectral decomposition and Filtered volume

This tool help for better imaging and mapping the temporal bed thickness and geological discontinuities within 3D seismic survey (Partyka et al., 1999) and also help seismic interpretation by identifying the variation of amplitude spectra and phase spectra. For this study I applied the latter one to image subtle faults in the interval of 1000-2000 msec. The seismic data were transferred into the frequency slices generated over a time windowed zone of interest. A band pass filter was determined for suitable range of frequencies (15, 20-30, 5 Hz) which the range was chosen based on the phase spectra of discrete frequencies that show subtle faults, which were not observed on conventional seismic.

Rock physics analysis

This tool was performed to identify suitable rock physics parameter to discriminate lithology and fluids. Crossplots of P-impedance and shale volume color coded by water saturation were examined to check the suitability of P-impedance to discriminate lithology and fluids.

Post-stack seismic inversion

Model based post-stack seismic inversion was executed to compute predicted P-impedance volume. I created initial P-impedance model from available log data and four interpreted horizons. Statistically estimated wavelet was used in inversion process. I also check the inverted P-impedance volume at well location

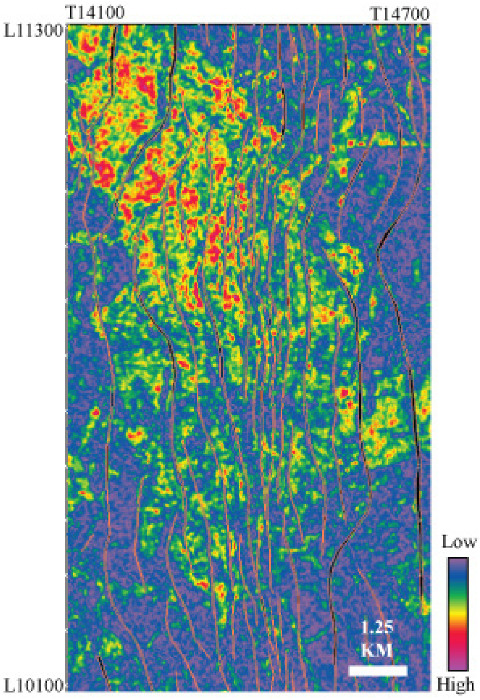

Figure 2. RMS map of H1 horizon.

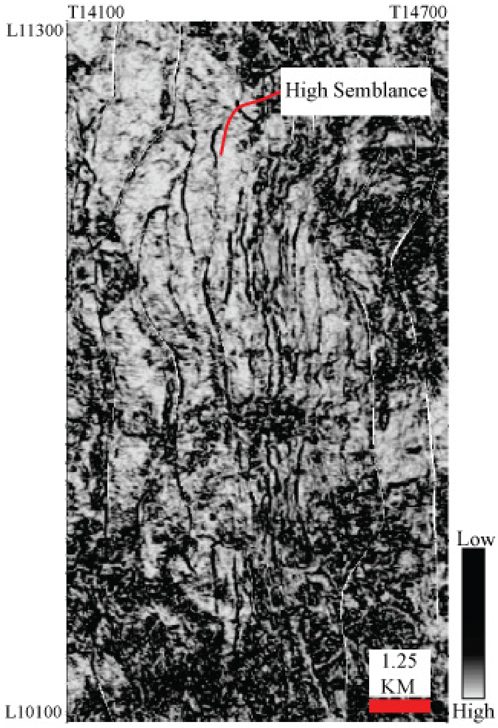

Figure 3. Semblance attribute map of H1 horizon.

4. Results

There are various results included RMS attribute analysis which I created from four horizons, RMS of H1 horizon is the representative of these results (Figure 2).

The semblance map of H1 horizon shows high semblance values are mostly along the northern part and trending Northwest-Southeastern (Figure 3).

Fault analysis was found that at the 26 Hz of iso-frequency time slice at 1000 msec and 1800 msec display the NW-SE oblique discontinuities in the northern part of the area and the southern part shows the SW-NE oblique discontinuities (Figure 4). The vertical section of filtered volume also shows these discontinuities (Figure 5).

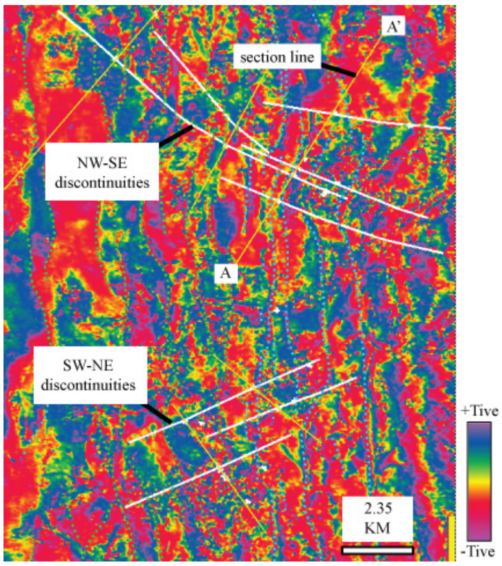

Figure 4. Example of time slice at 1000 msec generated from volume of 26 Hz iso-frequency phase spectra. NW-SE discontinuities located to the North and SW-NE discontinuities located to the south.

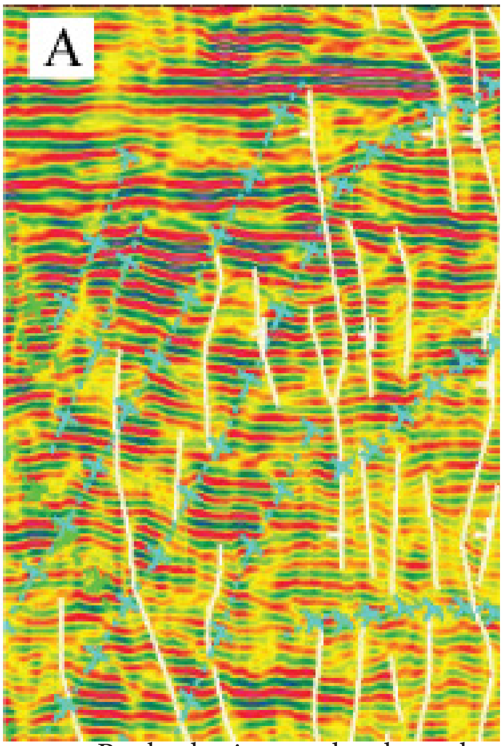

Figure 5. Example of Filtered section AA' across 1000 msec time slice of 26 Hz iso-frequency phase spectra. The white line is represent oblique discontinuities.

Rock physics results show that cross plot of P-impedance and shale volume can discriminate the high porosity sands (porosity > 24 %) from shale at the 6,500 m/s*g/cc. Moreover, color coded by water saturation can distinguish the clean sands that having gas from wet sands. The clean sands have less P-impedance and addition of gas in sands could make P-impedance further low (Figure 6).

QC of inversion output volume was performed by comparing original logs and inverted logs shows cross correlation of 87 %. The P-impedance logs were compared with computed section at well location. I chose the deviated well that show the low P-impedance of original log matches with low P-impedance, also low gamma ray values at well location are matching with low P-impedance (Figure 7). This is also supported by rock physics analysis, which indicated that sands have low P-impedance. Therefore, P-impedance volume can be successfully well to predict the sands between Middle Miocene intervals in this area.

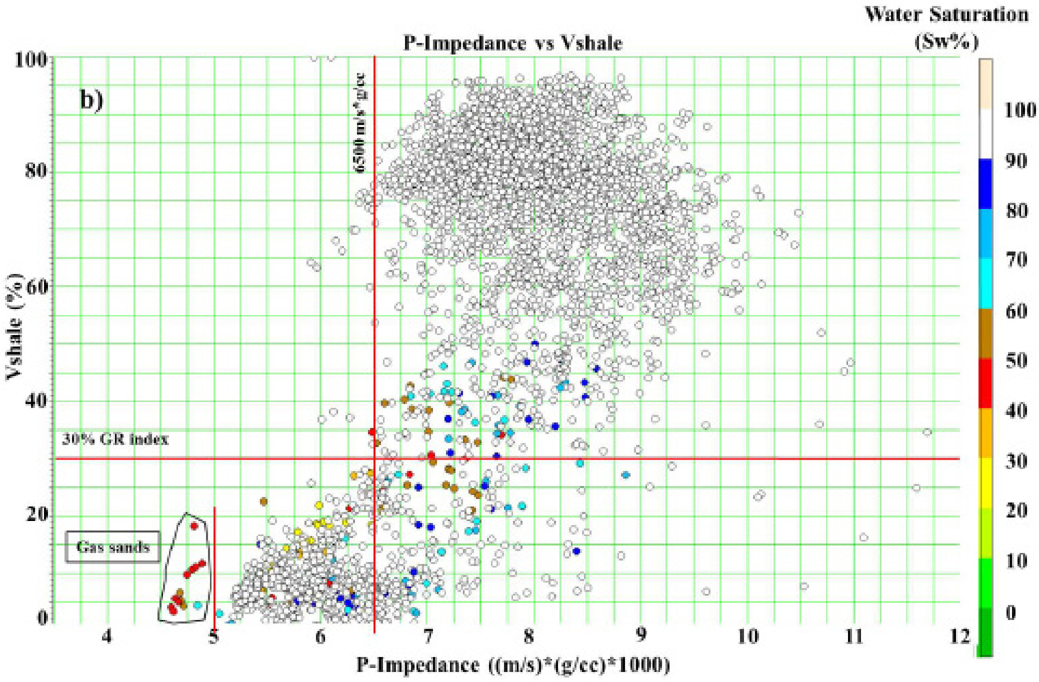

Figure 6. Cross plot of P-impedance and Vshale, color coded by water saturation.

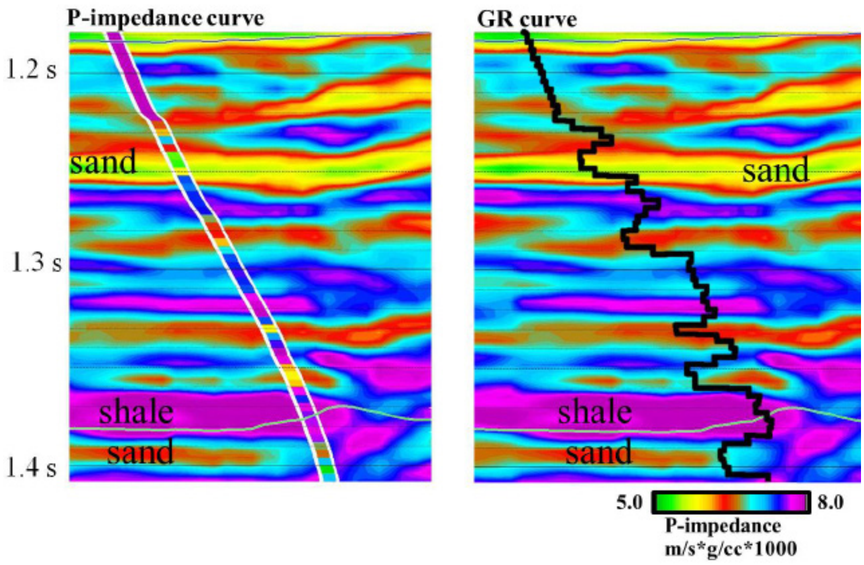

Figure 7. Inverted P-impedance section overlain by computed P-impedance curve (left) and gamma ray curve (right) along representative deviated well.

5. Discussion

High porosity sand distribution

According to Rock, physics analysis high porosity sands (greater than 24%) can be discriminated by P-impedance. two wells analyzed for rock physics show P-impedance range of 6500 to 7000 g/cc*m/s for high porosity sands.

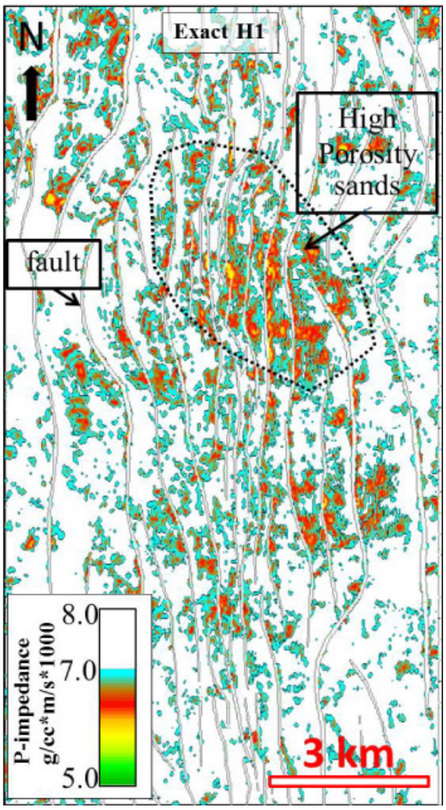

Figure 8. Map-view of the low values of acoustic impedance from post-stack inversion. The map was generated at exact H1 horizon.

The possible reason for variable range cutoff of P-impedance in different wells is different depth of zone of interest (between horizon B & C). I used cutoff of 7000 g/cc *m/s to image high porosity sands within the zone of interest. Low porosity sands have overlapping range of P-impedance with shale and cannot be discriminated based on P-impedance.

Low values of inverted acoustic impedance were extracted from post stack inversion volume along horizon surfaces to image the lateral distribution of the low P-impedance. Figure 8 shows the low P-impedance distribution map of low P-impedance at exact horizon location. As mentioned earlier than these low values of acoustic impedance are representing high porosity sands. The acoustic impedance outlook in the Figure 8, shows the interpretation of high porosity sands distribution at the exact horizon slices of H1 horizon. This map shows sands mostly exist along the up thrown side of normal fault, which is high side of these structural features. The high porosity located mostly at the northern part especially in the black dash circle in the Figure 8.

Well ER13 is within the high anomaly zone and log data of this well clearly shows thick sand at this level (Figure 9). Figure 9 shows low p-impedance map at H1 horizon GR log data of the well and cross section inverted P-impedance along the well ER13. This clearly shows that sand matches with low P-impedance values. High porosity sands show low P-impedance. Two blocky shape sands are observed near horizon H1. These are two stacked sands. These both stacked sands can be observed on the inverted section along the well. Figure 10 shows overlay of low P-impedance values over semblance horizon slice. Low P-impedance values matches with high semblance part. In

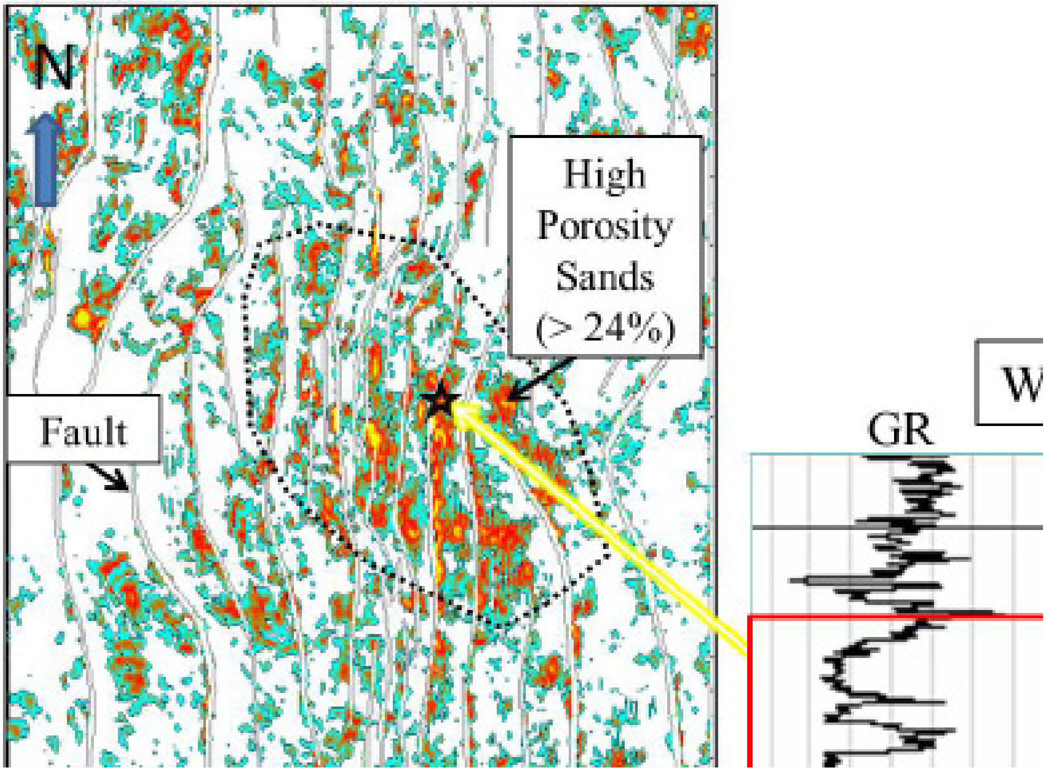

Figure 9. The P-impedance of high porosity sands at H1 horizon match with well log. The GR log shows sand stacking.

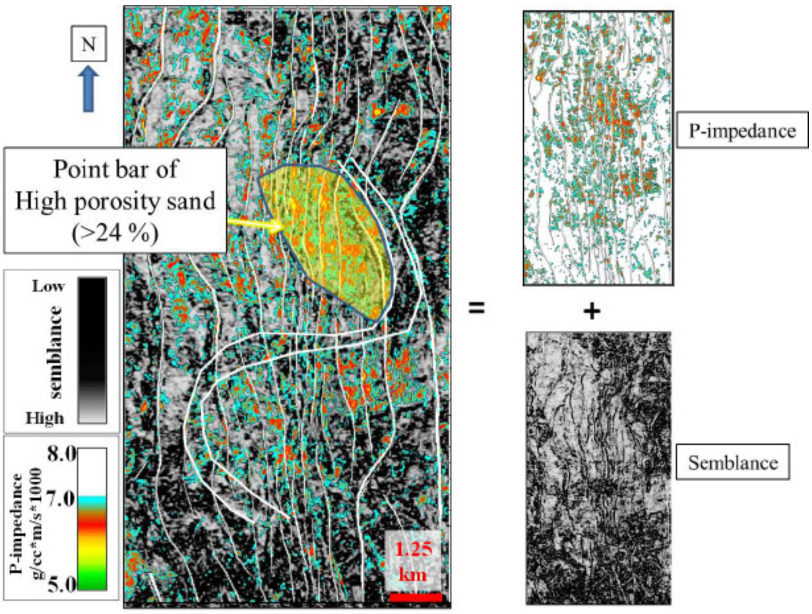

Figure 10. Very low P-impedance values superimposed on semblance. White line shows possible interpretation of channel and the yellow oval represents the point bar stacking sands.

the RMS analysis in the previous part, the RMS also shows same pattern of sands distribution. These high porosity (>24) sands are associated to low semblance sinuous feature on semblance horizon slice. Therefore, I suggest this zone possible to be point bar stacked sands (Figure 10). This workflow successfully predicts the sands associated with fluvial systems. These very low p-impedance values are mostly aligned with faults. These low impedance values may be due to gas presence, but based on the rock physics it is not easy to differentiate gas sands and water-wet sands by using P-impedance.

However, distribution pattern of these very low p-impedance values along faults may provide useful information about promising zones for gas exploration between horizon B and C. Rock physics analysis shows
that P-impedance is depth because of compaction. If we would be able to remove depth, we can get better image and interpret hydrocarbon with confident.

Structural interpretation and origin of oblique discontinuities

Some faults penetrate to the basement. On time slice, these oblique discontinuities are cross cutting the regional N-S faults. There are two possible reasons for these oblique discontinuities

1. Strike slip faulting associated with strike slip movement of regional faults such as Mae Ping, Three Pagoda fault and Ranong faults.

2. These are due to oblique extension influenced by pre-existing fabric.

According to Kornsawan and Morley, 2002 strike slip movement along major faults close to the gulf of Thailand was ceased before Oligocene. Therefore, these oblique discontinuities are not related with strike slip motion of regional faults. The other possible explanation of these discontinuities may be related with basement fabric, which is mostly oriented in NW-SE or
NE-SW direction in the Gulf of Thailand (Kornsawan and Morley, 2002; Morley et al., 2004). Figure 11 shows influence of pre-existing fabrics of strike slip faults that possible effect to the origin of oblique discontinuities. NW-SE oblique discontinuities zone may be influence from Three Pagoda fault and SW-NE oblique discontinuities zone may be influence from Ranong and Khlong Marui faults.

The relationship between the very low P-impedance and interpreted oblique discontinuities

Some very low P-impedance values are aligned along regional N-S faults. These very low anomalies of P-impedance may be because of hydrocarbon effect. Figure 12 shows overlay of interpreted oblique discontinuities on combined map of low P-impedance and RMS. It can be observed that some very low P-impedance values are also aligned along these oblique discontinuities. For this reason, it is significant to map these subtle NW-SE and
SW-NE discontinuities to comprehend the reservoir geometries, which could not be properly mapped on the conventional full spectrum seismic data. The

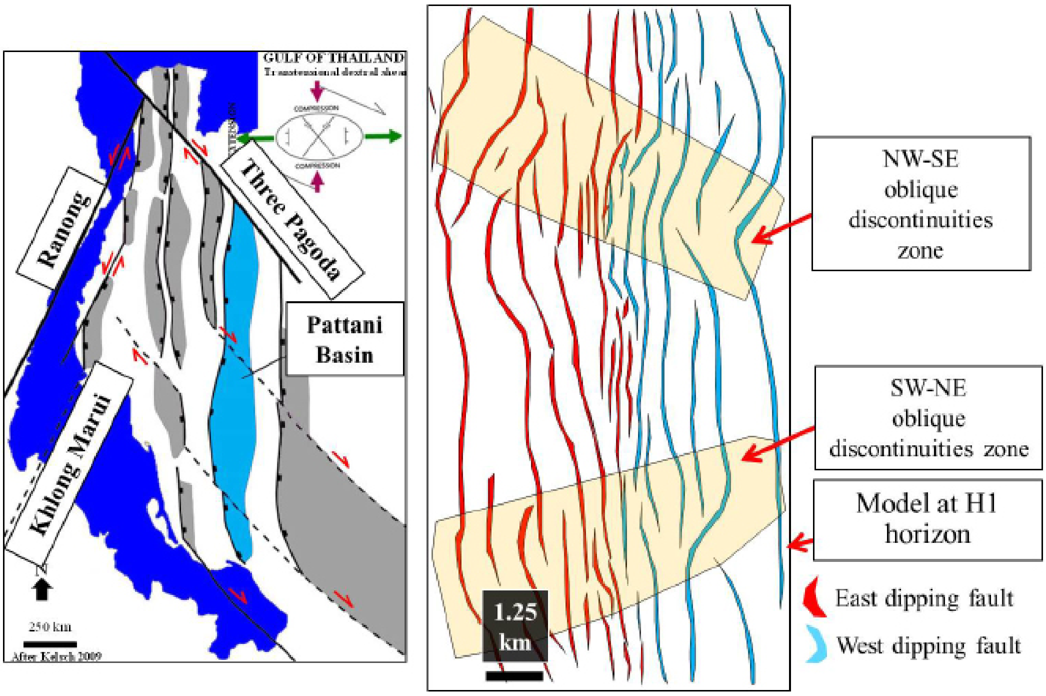

Figure 11. Llustration of relationship of strike-slip fault direction and oblique discontinuities direction in study area. The left: structural geology in the Gulf of Thailand. The right: model of oblique discontinuities represented by H1 structure map.

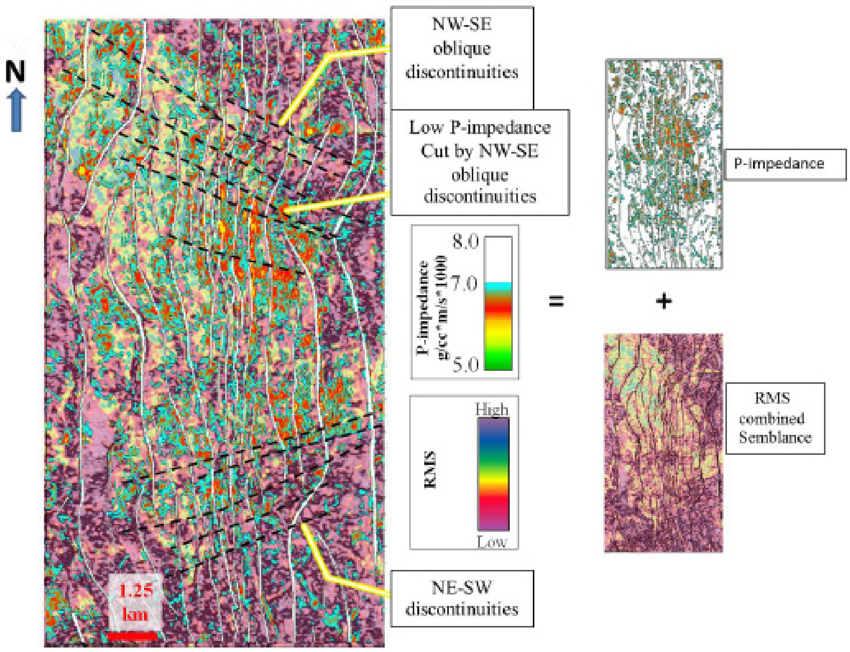

Figure 12. Low p-impedance overlay on RMS and semblance combined map. Blacked dashed lines are oblique discontinuities.

H1 horizon slice at the shallow section reveals that high amplitude output of RMS amplitude that calculated from conventional full spectrum seismic data and low P-impedance output of inversion P-impedance volume are associated with the following features

• High RMS amplitudes associated with low P-impedance. These are adjacent to the high structure of regional north south fault both west dipping and east-dipping as well as NW-SE and NE-SW discontinuities.

• Low RMS amplitudes associated with relatively high P-impedance away from high structure of faults (Figure 12)

High RMS amplitudes and low P-impedance associated with the oval shape as discussed in the previous (Figure 10) are interpreted as point bar stacked sand. This data from the shallow section might be helpful as analogous model for the deeper section of exploration, since the sediment deposition is prominently fluvial all over the depositional record of the basins in the Gulf of Thailand. Thereby, the high RMS amplitudes (represent sandstone) with low P-impedance (represent high porosity sandstone) and adjacent along the high structure of regional faults are more promising for the hydrocarbon exploration as compared to the low RMS amplitudes and relatively high P-impedance. Therefore, the RMS amplitudes associated with P-impedance inversion volume can help to map the reservoirs within the area more effectively as compared to the conventional full-spectrum seismic data at this interval study.

6. Conclusions

RMS amplitude, semblance, spectral decomposition (phase spectra), rock physics analysis and post stack seismic inversion techniques were applied to map the late Middle Miocene reservoir sands and subtle faults within Erawan area of the Pattani Basin. Main findings and conclusions are summarized below;

• Semblance and phase spectra of spectral decomposition can successfully map discontinuities related with graben shifts or transfer zones in Erawan area.

• Discontinuities associated with NW-SE and NE-SW subtle faults are compartmentalizing the reservoir sands. Therefore, mapping of these oblique discontinuities is useful for exploration and production.

• These oblique discontinuities at some places are penetrating to basement and may be related with pre-rift basement fabric.

• According to rock physics analysis acoustic impedance can differentiate high porosity (>24%) sands from shale.

• High gas saturated clean sands can also be differentiated from water-wet sands. However, this is not always easy as acoustic impedance increases with increase of shale percentage and we observe overlapping range of acoustic impedance for gas saturated silty sands and water-wet clean sands.

• Very low acoustic impedance anomalies are observed along regional N-S faults and oblique discontinuities. These very low acoustic impedance anomalies may be considered potential target for future exploration.

Acknowledgments

I would like to thank my supervisor Dr. Mirza Naseer Ahmad for his valuable comments and discussions also precious support and honorable suggestions in every part of my final research project. In addition, I would like to thank Prof. Joseph Lambiase, Prof. Phillip Rowell and Prof. John Warren for their fundamental knowledge through the Petroleum Geoscience Program. I like to thank Landmark Graphics and CGG for providing academic licenses of software. I also thank to my company supervisors, Mr. Jim Logan, Mr. Lance D. Brunsvold, Mr. Natthawut Charoenthanwa, Mr. Roger Griffith.

References

Crossley, A.R., 1990. The Geology and hydrocarbon potential of the Pattani basin. Gulf of Thailand, unpublished research, Unocal Thailand, 5-64.

Jardine, E., 1997. Dual petroleum systems governing the prolific Pattani Basin, offshore Thailand. Petroleum systems of S.E. Asia and Australasia Conference, Jakarta, May 21-23, 1997, p. 351-363.

Kornsawan, A., and C. K. Morley, 2002, The origin and evolution of complex transfer zones (graben shifts) in conjugate fault systems around the Funan Field, Pattani Basin, Gulf of Thailand: Journal of Structural Geology, v. 24,p. 435-449.

Morley, C. K., C. Haranya, W. Phoosongsee, S. Pongwapee, A. Kornsawan, and N. Wonganan, 2004, Activation of rift oblique and rift parallel pre-existing fabrics during extension and their effect on deformation style: examples from the rifts of Thailand: Journal of Structural Geology, v. 26, p. 1803-1829.

Morley, C. K., and A. Racey, 2011, Tertiary stratigraphy, in M. F. Ridd, A. J. Barber, and M. J. Crow, The Geology of Thailand: London, Geological Society, p.223-272.

Partyka, G.A., Gridly, J.M., and Lopez, J. 1999, International Applications of Special Decomposition in Reservoir Characterization, The Leading Edge, vol. 18, No. 3, p.353-360.

Watcharanantakul, R., and Morley, C. K., 2000. Syn-rift and post-rift modeling of the Pattani Basin, Thailand: evidence for a ramp-flat detachment. Marine and Petroleum Geology, v.17, p. 937-958.